Supplementary Information (SI) for Journal of Materials Chemistry A.

Supplementary Information

Designing High-Performance Catalysts for Urea Electrosynthesis: Synergy between Single Atoms and BC_3 Monolayers

Wanying Guo, [a,#] *Yuwei Yan,* [a,#] *Zhenghaoyang Zhu,* [a] *Yuejie Liu,*[b,*] *Jingxiang Zhao*[a,*]

[a] *Key Laboratory of Photonic and Electronic Bandgap Materials, Ministry of Education, School of Physics and Electronic Engineering, College of Chemistry and Chemical Engineering, Harbin Normal University, Harbin, 150025, China*

[b] *Modern Experiment Center, Harbin Normal University, Harbin, 150025, China.*

[*] *To whom correspondence should be addressed. Email: liuyuejie@hrbnu.edu.cn; zhaojingxiang@hrbnu.edu.cn (J.Z.)*

[#] *Wanying Guo and Yuwei Yan contributed equally to this work.*

Computational Details

The computational hydrogen electrode (CHE) model

The Gibbs free energy change (ΔG) for each elementary step was computed using the computational hydrogen electrode (CHE) model, which is defined by: $\Delta G = \Delta E + \Delta ZPE - T\Delta S + eU$ where ΔE is the reaction energy of reactant and product species adsorbed on the catalyst directly obtained from DFT computations; ΔZPE and ΔS represent the differences in zero-point energy and entropy, respectively, between the adsorbed species and the gas phase molecules at 298.15 K, which can be calculated from the vibrational frequencies, U is the applied potentials. To evaluate the activity of different candidate compounds in urea synthesis, the limiting potential (U_L) was computed by: $U_L = -\max(\Delta G_1, \Delta G_2, \Delta G_3, \Delta G_4 \ldots\ldots, \Delta G_i)/e$, where ΔG_i is the free energy change of each elementary step in the whole process, in which a less negative U_L suggests a low energy input, thus demonstrating its higher catalytic activity.

Table S1. The all computed free energy changes (ΔG, eV) of the possible different reaction mechanisms involved in urea synthesis. The ΔG values of the selected steps are remarked in red.[a]

Elementary step	ΔG
$2N_2 + {}^{*} \rightarrow {}^{*}N_2N_2^{\#}$	-0.95
$^{*}N_2N_2^{\#} + CO \rightarrow {}^{*}N_2CON_2^{\#}$	0.28
$^{*}N_2CON_2^{\#} + H^+ + e^- \rightarrow {}^{*}N_2HCON_2^{\#}$	0.17
$^{*}N_2CON_2^{\#} + H^+ + e^- \rightarrow {}^{*}NHNCON_2^{\#}$	0.67
$^{*}N_2CON_2^{\#} + H^+ + e^- \rightarrow {}^{*}N_2CHON_2^{\#}$	0.62
$^{*}N_2CON_2^{\#} + H^+ + e^- \rightarrow {}^{*}N_2COHN_2^{\#}$	0.97
$^{*}N_2HCON_2^{\#} + H^+ + e^- \rightarrow {}^{*}N_2HCON_2H^{\#}$	0.16
$^{*}N_2HCON_2^{\#} + H^+ + e^- \rightarrow {}^{*}NHNHCON_2^{\#}$	0.82
$^{*}N_2HCON_2^{\#} + H^+ + e^- \rightarrow {}^{*}N_2HCONHN^{\#}$	0.97
$^{*}N_2HCON_2H^{\#} + H^+ + e^- \rightarrow {}^{*}N_2HCONHNH^{\#}$	-0.61
$^{*}N_2HCON_2H^{\#} + H^+ + e^- \rightarrow {}^{*}NNH_2CON_2H^{\#}$	-2.13
$^{*}N_2HCONHNH^{\#} + H^+ + e^- \rightarrow {}^{*}N_2HCONHNH_2^{\#}$	-0.06
$^{*}N_2HCONHNH^{\#} + H^+ + e^- \rightarrow {}^{*}NNH_2CONHNH^{\#}$	1.27
$^{*}N_2HCONHNH^{\#} + H^+ + e^- \rightarrow {}^{*}N_2HCONH_2NH^{\#}$	-1.86
$^{*}NNH_2CON_2H^{\#} + H^+ + e^- \rightarrow {}^{*}NNH_2CONHNH^{\#}$	-2.72
$^{*}N_2HCONHNH_2^{\#} + H^+ + e^- \rightarrow {}^{*}N_2HCONH^{\#} + NH_3$	-1.69
$^{*}N_2HCONHNH_2^{\#} + H^+ + e^- \rightarrow {}^{*}NHNHCONHNH_2^{\#}$	0.10
$^{*}N_2HCONHNH_2^{\#} + H^+ + e^- \rightarrow {}^{*}NNH_2CONHNH_2^{\#}$	-2.57
$^{*}N_2HCONH_2NH^{\#} + H^+ + e^- \rightarrow {}^{*}N_2HCONH_2NH_2^{\#}$	-1.17
$^{*}NNH_2CONHNH^{\#} + H^+ + e^- \rightarrow {}^{*}NHNH_2CONHNH^{\#}$	1.01
$^{*}N_2HCONH^{\#} + H^+ + e^- \rightarrow {}^{*}NHNHCONH^{\#}$	-0.44
$^{*}N_2HCONH^{\#} + H^+ + e^- \rightarrow {}^{*}N_2HCONH_2^{\#}$	0.22
$^{*}N_2HCONH^{\#} + H^+ + e^- \rightarrow {}^{*}NNH_2CONH^{\#}$	0.14
$^{*}NNH_2CONHNH_2^{\#} + H^+ + e^- \rightarrow {}^{*}NNH_2CONH^{\#} + NH_3$	1.02
$^{*}N_2HCONH_2NH_2^{\#} + H^+ + e^- \rightarrow {}^{*}NHNHCONH_2NH_2^{\#}$	-0.35
$^{*}NHNH_2CONHNH^{\#} + H^+ + e^- \rightarrow {}^{*}NH_2NH_2CONHNH^{\#}$	0.41
$^{*}NHNHCONH^{\#} + H^+ + e^- \rightarrow {}^{*}NHNHCONH_2^{\#}$	0.47
$^{*}NHNHCONH^{\#} + H^+ + e^- \rightarrow {}^{*}NH_2NHCONH^{\#}$	1.43
$^{*}NHNHCONH^{\#} + H^+ + e^- \rightarrow {}^{*}NHNH_2CONH^{\#}$	0.54
$^{*}NNH_2CONH^{\#} + H^+ + e^- \rightarrow {}^{*}NHNHCONH_2^{\#}$	-0.11
$^{*}NHNHCONH_2NH_2^{\#} + H^+ + e^- \rightarrow {}^{*}NH_2NHCONH_2NH_2^{\#}$	1.15
$^{*}NH_2NH_2CONHNH^{\#} + H^+ + e^- \rightarrow {}^{*}NH_2CONHNH^{\#} + NH_3$	1.10
$^{*}NHNHCONH_2^{\#} + H^+ + e^- \rightarrow {}^{*}NH_2NHCONH_2^{\#}$	-0.28
$^{*}NHNHCONH_2^{\#} + H^+ + e^- \rightarrow {}^{*}NHNH_2CONH_2^{\#}$	1.39
$^{*}NH_2NHCONH_2NH_2^{\#} + H^+ + e^- \rightarrow {}^{*}NH_2NHCONH_2^{\#} + NH_3$	0.23
$^{*}NH_2NHCONH_2^{\#} + H^+ + e^- \rightarrow {}^{*}NHCONH_2^{\#} + NH_3$	-0.69
$^{*}NHCONH_2^{\#} + H^+ + e^- \rightarrow {}^{*}NH_2CONH_2^{\#}$	0.17

$^{*}NH_2CONH_2{}^{\#} \rightarrow {}^{*} + NH_2CONH_2$	1.78

[a] It should be noted that, although some elementary steps exhibit lower free energy changes, their further hydrogenation may require lager energy input. For example, the steps from $^{*}N_2HCON_2H^{\#}$ to $*NNH_2CON_2H^{\#}$, and $^{*}NNH_2CONHNH^{\#}$ have relatively negative free energy changes of -2.13 and -2.57 eV, respectively. However, the further hydrogenation of $^{*}NNH_2CONHNH^{\#}$ is difficult due to its high free energy change of 1.01 eV, which is consistent with the famous Sabatier principle, namely, the too strong or too weak adsorption of reaction intermediates on the catalyst will lead to poor catalytic performance.

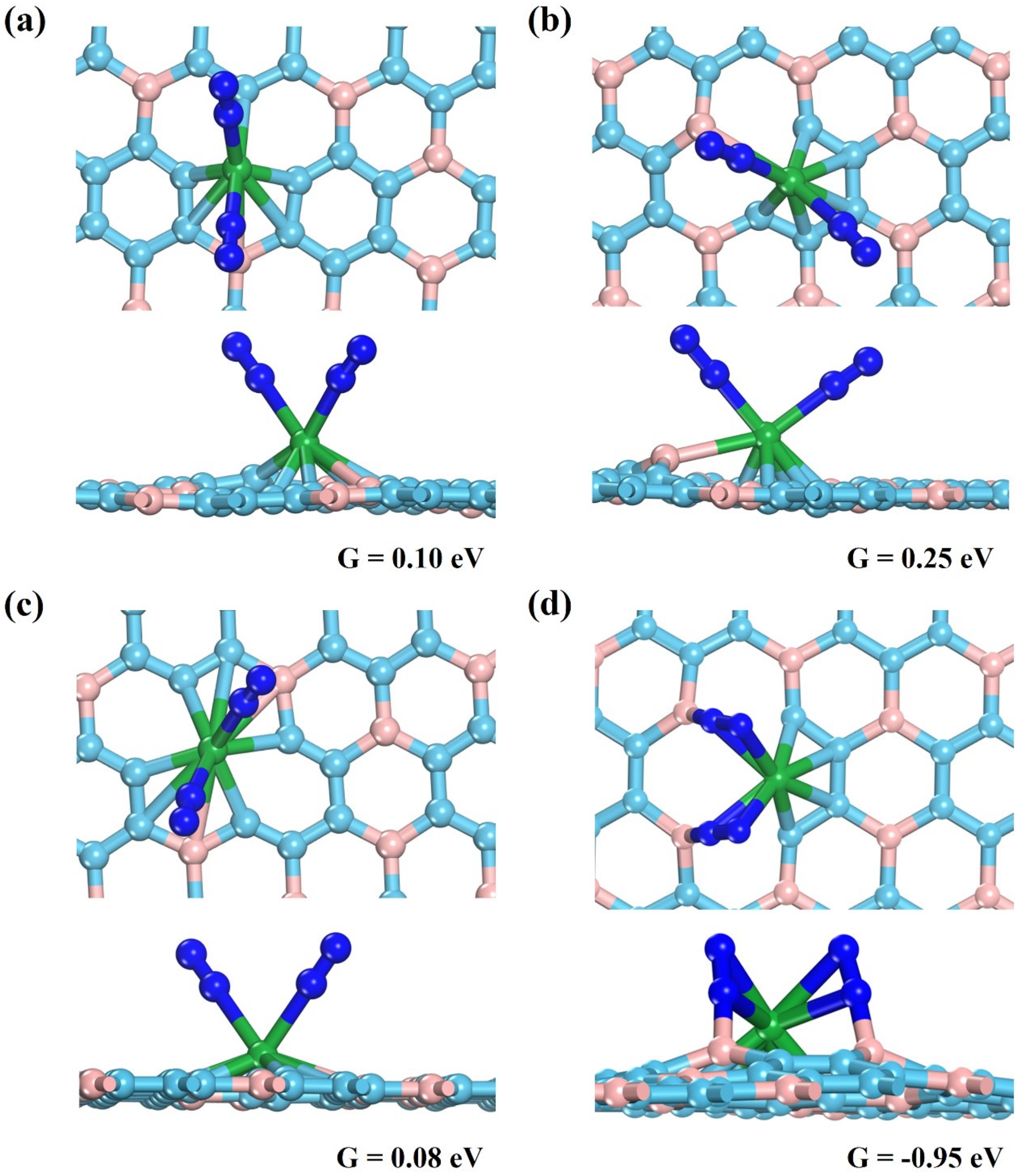

Fig. S1. Optimize the adsorption of two N_2 molecules on structures with the removal of different proportions of vacancies BC_3 (a) with B vacancy, (b) with C vacancy, (c) with B–C double vacancies, and (d) with C–C double vacancies. Only C–C dual vacancies can adsorb two N_2 molecules in a side-on form with the lowest energy.

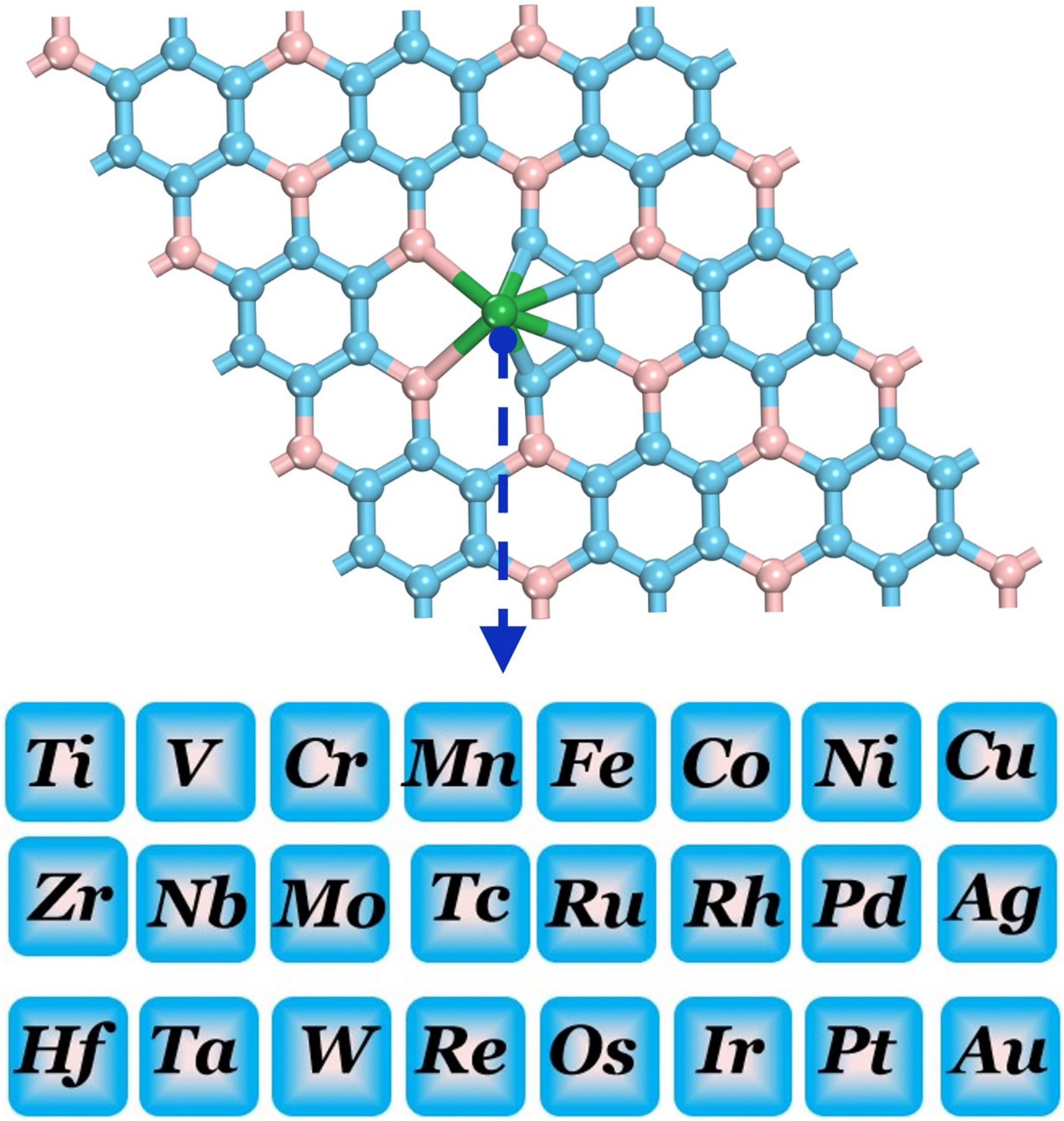

Fig. S2. The considered SACs anchored on BC_3 nanosheets with C-C vacancy.

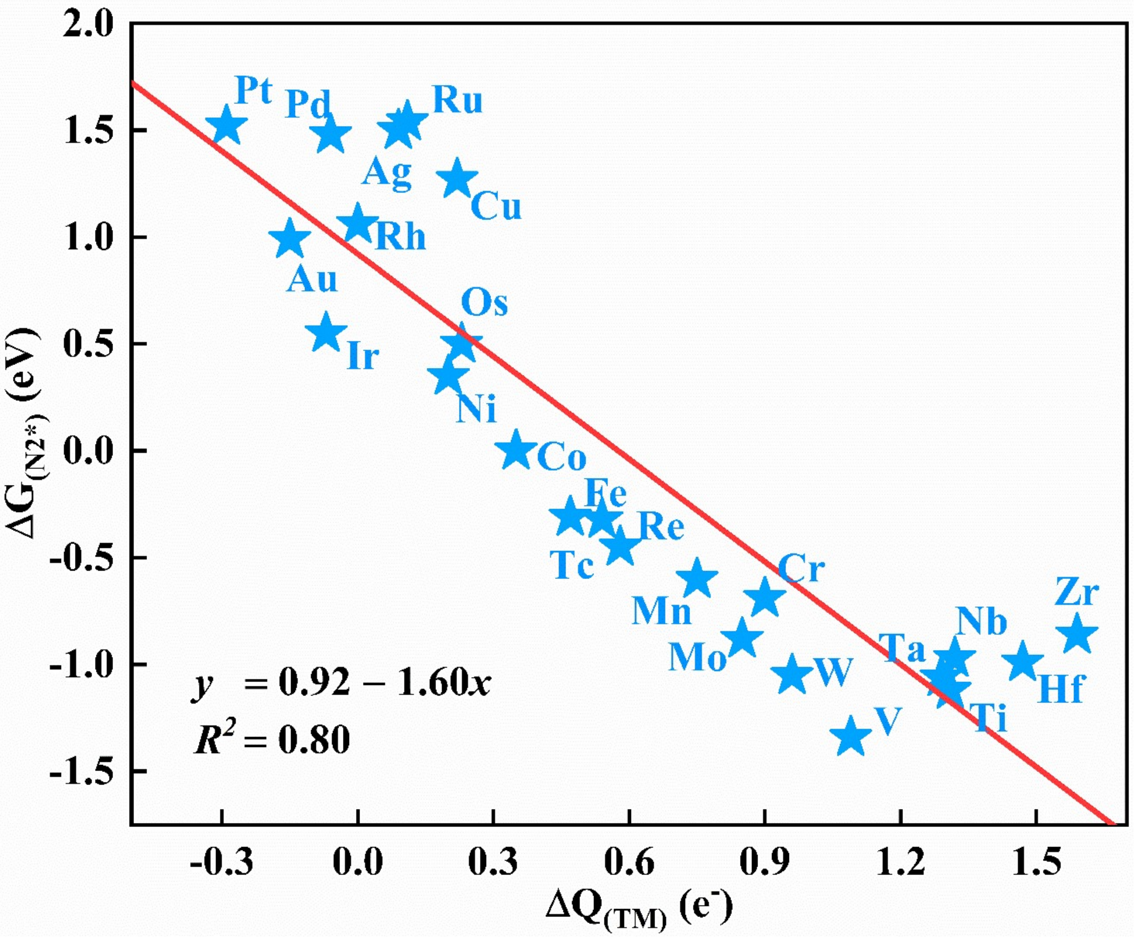

Fig. S3. The linear relationship between charges (ΔQ_{TM}) of the active sites and the free adsorption energies (ΔG_{N2*}) of N_2 molecule.

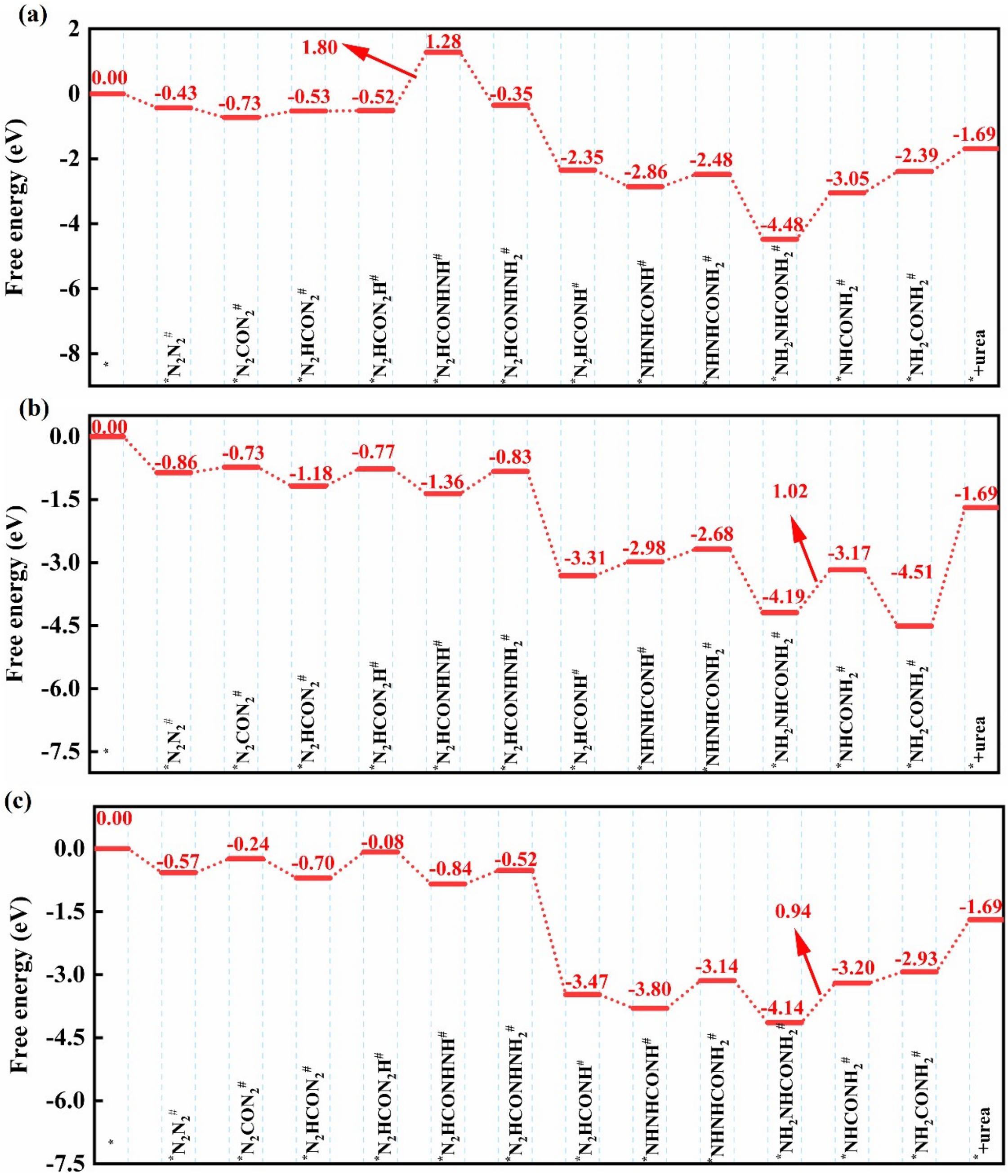
(a)
Free energy (eV)
2
0
-2
-4
-6
-8
0.00
-0.43
-0.73
-0.53
-0.52
1.28
1.80
-0.35
-2.35
-2.86
-2.48
-4.48
-3.05
-2.39
-1.69
*
*N2N2#
*N2CON2#
*N2HCON2#
*N2HCON2H#
*N2HCONHNH#
*N2HCONHNH2#
*N2HCONH#
*NHNHCONH#
*NHNHCONH2#
*NH2NHCONH2#
*NHCONH2#
*NH2CONH2#
*+urea
(b)
Free energy (eV)
0.0
-1.5
-3.0
-4.5
-6.0
-7.5
0.00
-0.86
-0.73
-1.18
-0.77
-1.36
-0.83
-3.31
-2.98
-2.68
-4.19
1.02
-3.17
-4.51
-1.69
(c)
Free energy (eV)
0.0
-1.5
-3.0
-4.5
-6.0
-7.5
0.00
-0.57
-0.24
-0.70
-0.08
-0.84
-0.52
-3.47
-3.80
-3.14
-4.14
0.94
-3.20
-2.93
-1.69

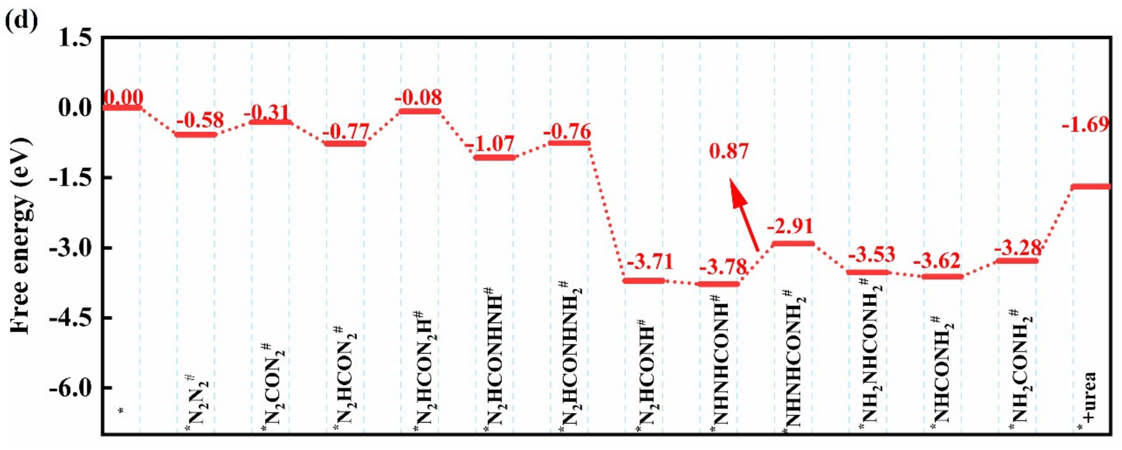

Fig. S4. The free energy profile for urea electrosynthesis on (a) Ti/BC_3, (b) V/BC_3, (c) Nb/BC_3, and (d) Ta/BC_3, along with the free energy changes of each elementary step.

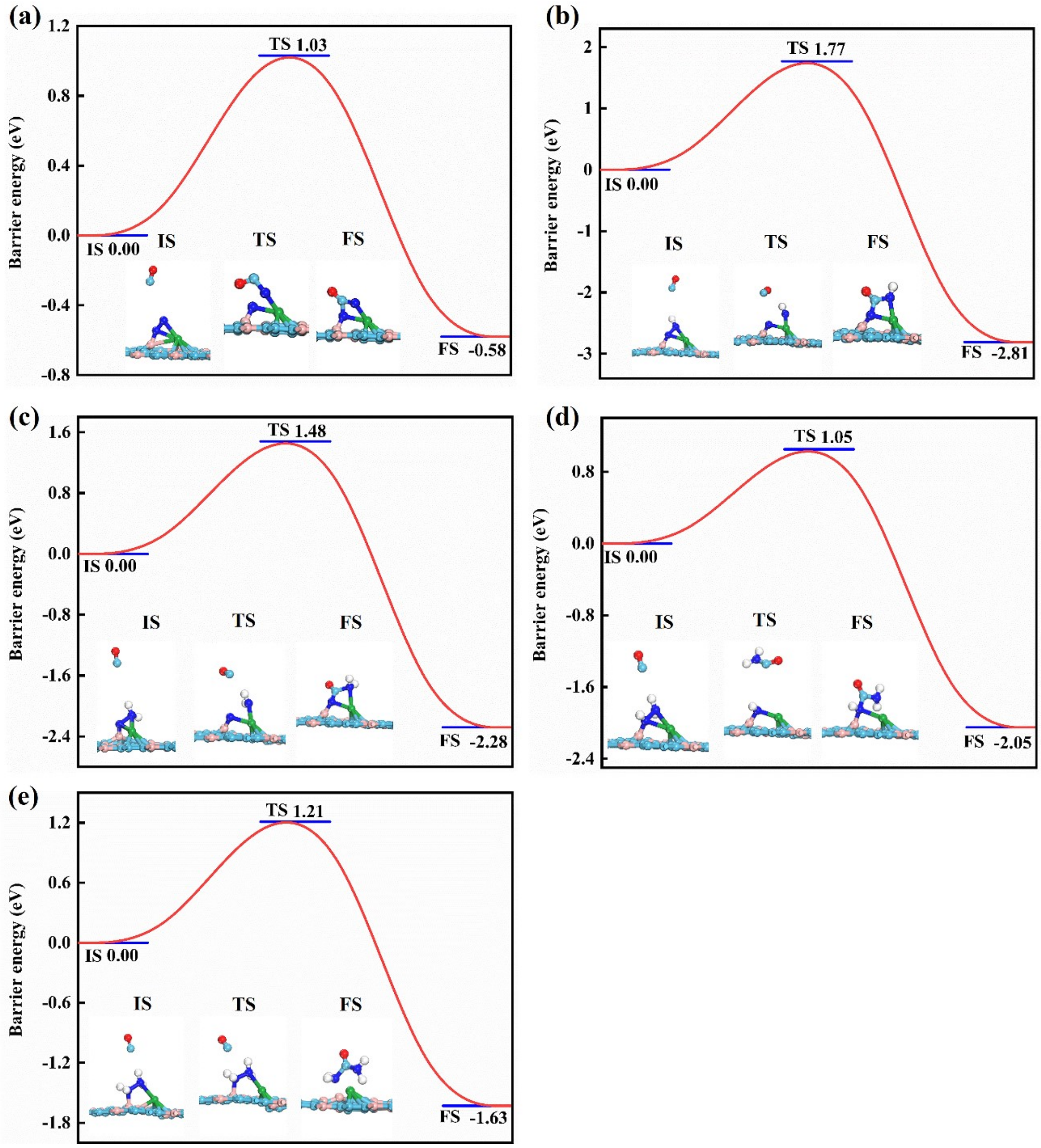

Fig. S5. The kinetic barriers and structures for CO insertion into a single adsorbed (a) $^{*}N_2$ molecule along with its hydrogenated intermediates, including (b) $^{*}N_2H$, (c) $^{*}N_2H_2$, (d) $^{*}N_2H_3$, and (e) $^{*}N_2H_4$.

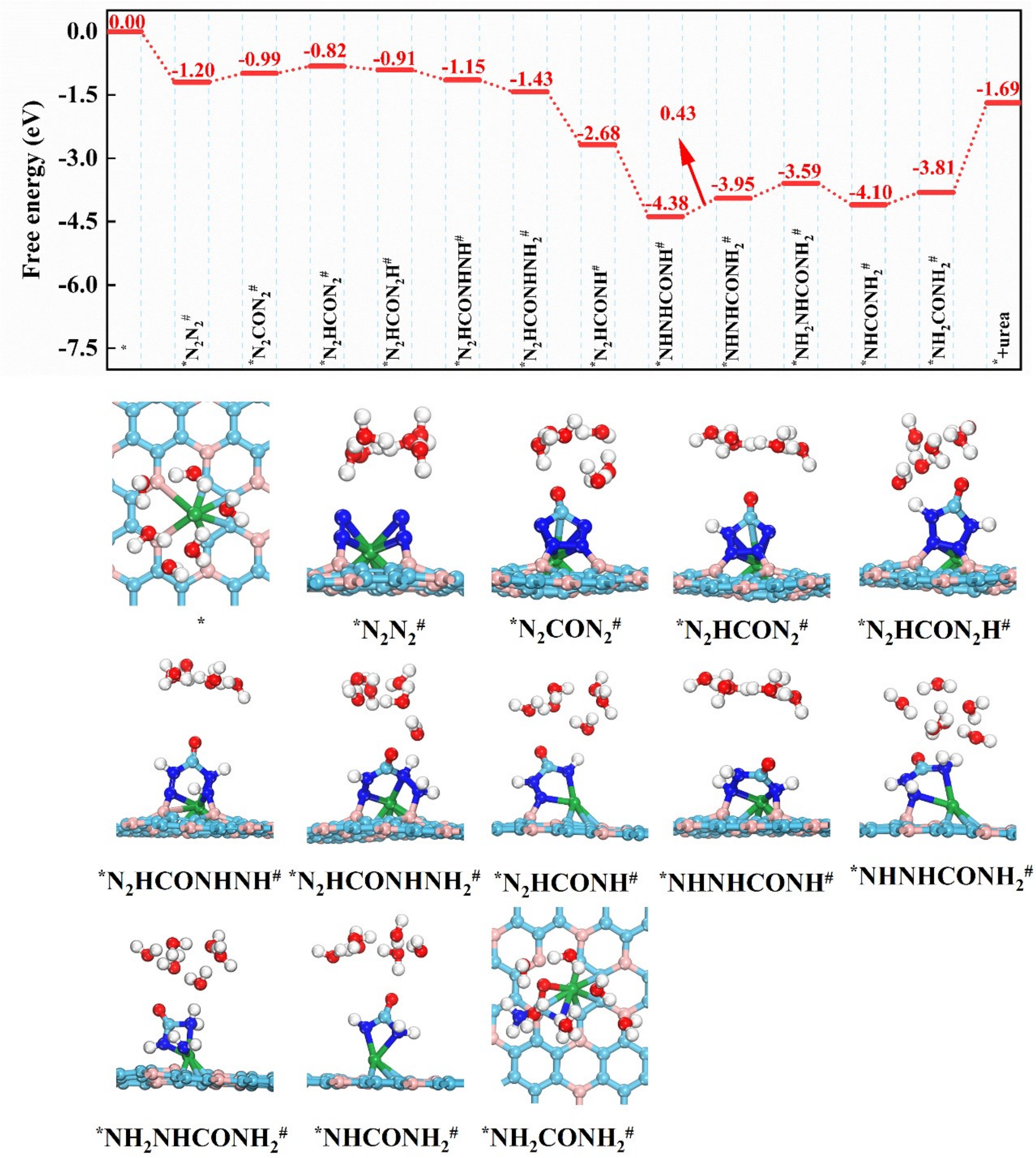

Fig. S6. The free energy profile and structures for urea electrosynthesis using an explicit solvent model on the Hf/BC_3 catalyst.

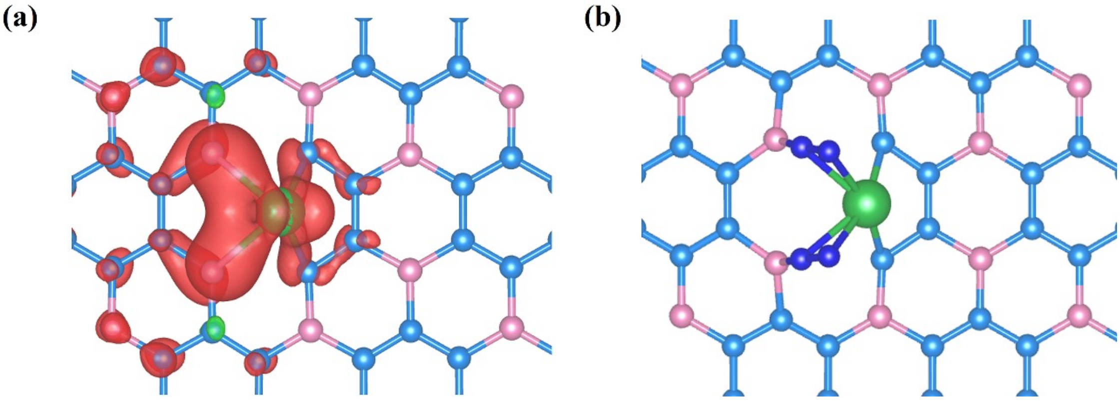

Fig. S7. (a) Spin−resolved density isosurfaces of Hf/BC_3 catalyst. (b) $2N_2$ adsorbs on the spin decomposition density equipotential surface of the Hf/BC_3 catalyst. The isovalue was set to be 0.0025 eÅ^{-2}.

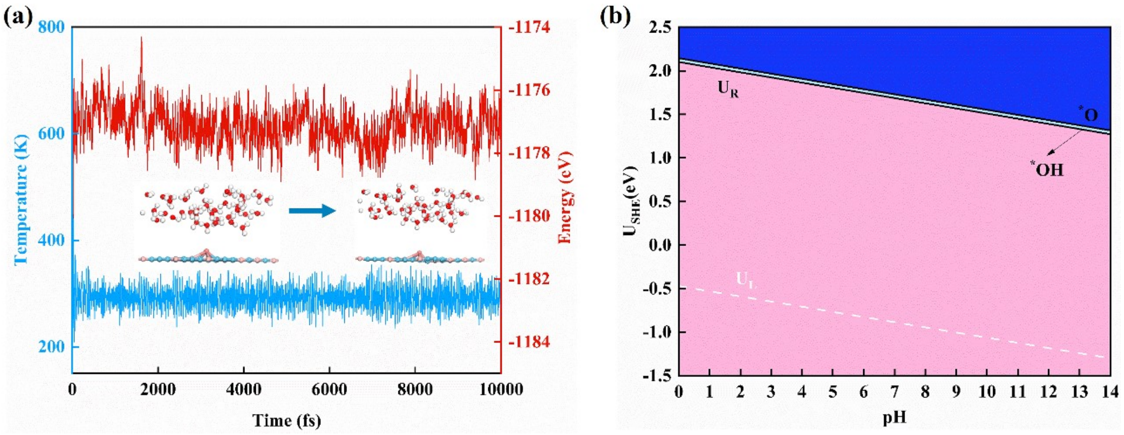

Fig. S8. (a) The ab initio molecular dynamics (AIMD) simulations for a total of 10 ps to assess the stability of the Hf/BC$_3$ catalyst at 300 K under aqueous conditions, as modeled with a 40-molecule water layer. (b) The surface Pourbaix diagram of Hf/BC$_3$.